

# Mechanism of Cycloaddition Reactions between Ketene and *N*-Silyl-, *N*-Germyl-, and *N*-Stannylimines: A Theoretical Investigation

Pablo Campomanes, M. Isabel Menéndez, and Tomás L. Sordo\*

Departamento de Química Física y Analítica, Facultad de Química, Universidad de Oviedo, C/Julián Clavería, 8, 33006 Oviedo, Principado de Asturias, Spain

Received: July 25, 2005; In Final Form: October 17, 2005

A theoretical study of the cycloaddition reactions of ketene and *N*-silyl-, *N*-germyl-, and *N*-stannylimines were performed at the B3LYP/6-311+G(d,p) theory level using the LANL2DZ effective core potential for Ge and Sn and taking into account the effect of diethyl ether solvent by means of the polarizable continuum model method. According to the obtained results the reaction between ketene and *N*-germylimine is a two-step process due to the effect of solvent, whereas the cycloaddition of ketene and *N*-silylimine follows a three-step mechanism because in this case the evolution of the electronic energy along the reaction coordinate predominates over the effect of solvent. For *N*-stannylimine the two- and three-step mechanisms are competitive. In all the cases the rate-determining barrier corresponds to the evolution of the azadiene intermediate. The cycloaddition of ketene and *N*-germylimine is kinetically the most favorable reaction of the three studied by us and can take place as a domino process. In the three cases the isomerization of the imine through the inversion at the nitrogen atom is easier than the formation of the azadiene intermediate so that the three processes would afford the *trans*- $\beta$ -lactam.

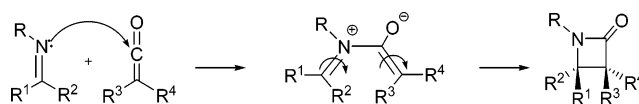
## Introduction

Among the numerous methods for the synthesis of  $\beta$ -lactams, the cycloaddition reaction of ketenes with imines, known as the Staudinger reaction, has proven to be a versatile procedure for the construction of the  $\beta$ -lactam ring.<sup>1</sup> The mechanism of the reaction involves the nucleophilic attack of the lone pair of the nitrogen atom of an imine on the central carbon atom of a ketene and subsequent conrotatory electrocyclicization of the resultant zwitterionic intermediate leading to a  $\beta$ -lactam whose stereochemistry can be *cis*, *trans*, or a mixture of both isomers (Scheme 1).<sup>2</sup> This mechanism is based both on experimental evidence of the occurrence of a zwitterionic intermediate<sup>3</sup> and on theoretical studies.<sup>4</sup>

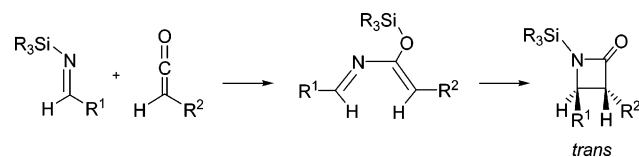
It has been reported that *trans*- $\beta$ -lactams have been obtained through the Staudinger reactions of ketenes and *N*-silylimines (Scheme 2).<sup>5</sup> This is clearly a formal two-step Staudinger reaction since *O*-silylated intermediates have been isolated. Theoretical studies have also been performed on this process showing that the formation of the  $\beta$ -lactam ring takes place through two consecutive reactions.<sup>6</sup> The first one consists of the nucleophilic addition of the iminic nitrogen to the central carbon atom of the ketene, with simultaneous migration of the silyl group from the imine to the oxygen atom of the ketene to form silyl-enol intermediates. Formation of the *N*-silylated  $\beta$ -lactam takes place via a domino reaction<sup>7</sup> consisting of a conrotatory electrocyclicization followed by a new silatropic rearrangement. The rationalization of how *trans*- $\beta$ -lactams are obtained is possible because the energy barrier for the isomerization of the initial *N*-silylimine is lower than that associated with the formation of the C–N bond.

Given that according to theoretical studies<sup>8</sup> the activation barriers for 1,3-migration of MH<sub>3</sub> groups (M = C, Si, Ge, Sn)

## SCHEME 1



## SCHEME 2



decrease when going down the 14 group we planned to investigate the effect of this different facility of migration on the mechanism of the cycloaddition reactions of ketene with *N*-silyl-, *N*-germyl-, and *N*-stannylimines.

## Computational Methods

Full geometry optimizations were performed with the B3LYP density functional method (DFT),<sup>9</sup> using the 6-311+G(d,p) basis set for H, C, N, O, and Si atoms, and the effective core potential LANL2DZ<sup>10</sup> for Ge and Sn atoms both in gas phase and in solution. All calculations were carried out with the Gaussian03 series of programs.<sup>11</sup> The nature of the stationary points located was further checked, and zero point vibrational energies (ZPVE) were evaluated by analytical computations of harmonic vibrational frequencies at the same theory level. Intrinsic reaction coordinate (IRC) calculations were also carried out to check the connection between the transition states (TSs) and the minimum energy structures using the Gonzalez and Schlegel method<sup>12</sup> implemented in Gaussian03.

$\Delta G_{\text{gas}}$  values were also calculated within the ideal gas, rigid rotor, and harmonic oscillator approximations.<sup>13</sup> A pressure of 1 atm and a temperature of 298.15 K were assumed in the calculations.

\* To whom correspondence should be addressed. E-mail: tsordo@uniovi.es.

**TABLE 1:** Relative B3LYP Electronic Energies and Gibbs Energies in Solution (kcal mol<sup>-1</sup>) for the Critical Structures Located along the Reaction Coordinates for the Three Studied Cycloadditions and for the Isomerization of the Corresponding Imines<sup>a</sup>

structures	$\Delta E_{\text{elec}}$			$\Delta G_{\text{solution}}$		
	Si	Ge	Sn	Si	Ge	Sn
<b>R</b>	0.0	0.0 (0.0)	0.0	0.0	0.0 (0.0)	0.0
<b>TSR1</b>	8.2	4.6 (5.9)	1.2	19.3	16.1 (17.2)	13.4
<b>I1</b>	-19.7	-17.3 (-15.7)	-22.5	-4.1	-1.9 (-0.4)	-6.8
<b>TS12</b>	14.0	15.3 (16.9)	10.6	27.6	29.0 (30.5)	24.5
<b>I2</b>	-22.7	-22.1 (-20.3)	-27.2	-8.3	-7.6 (-6.0)	-12.4
<b>TS2P</b>	-0.2	-6.7 (-4.2)	-21.5	13.3	7.6 (10.0)	-6.6
<b>TS1P</b>	18.1	15.7 (17.3)	13.2	29.0	26.8 (28.2)	24.6
<b>P</b>	-35.7	-37.0 (-35.3)	-38.8	-23.4	-24.2 (-22.4)	-25.1
ketene + <b>TS<sub>inv</sub></b>	7.1	11.6 (12.8)	8.6	7.3	11.8 (12.9)	8.9

<sup>a</sup> In parentheses are given the results obtained for *N*-germylimine at the B3LYP/6-311+G(d,p) theory level through full geometry optimization in gas phase and in solution.

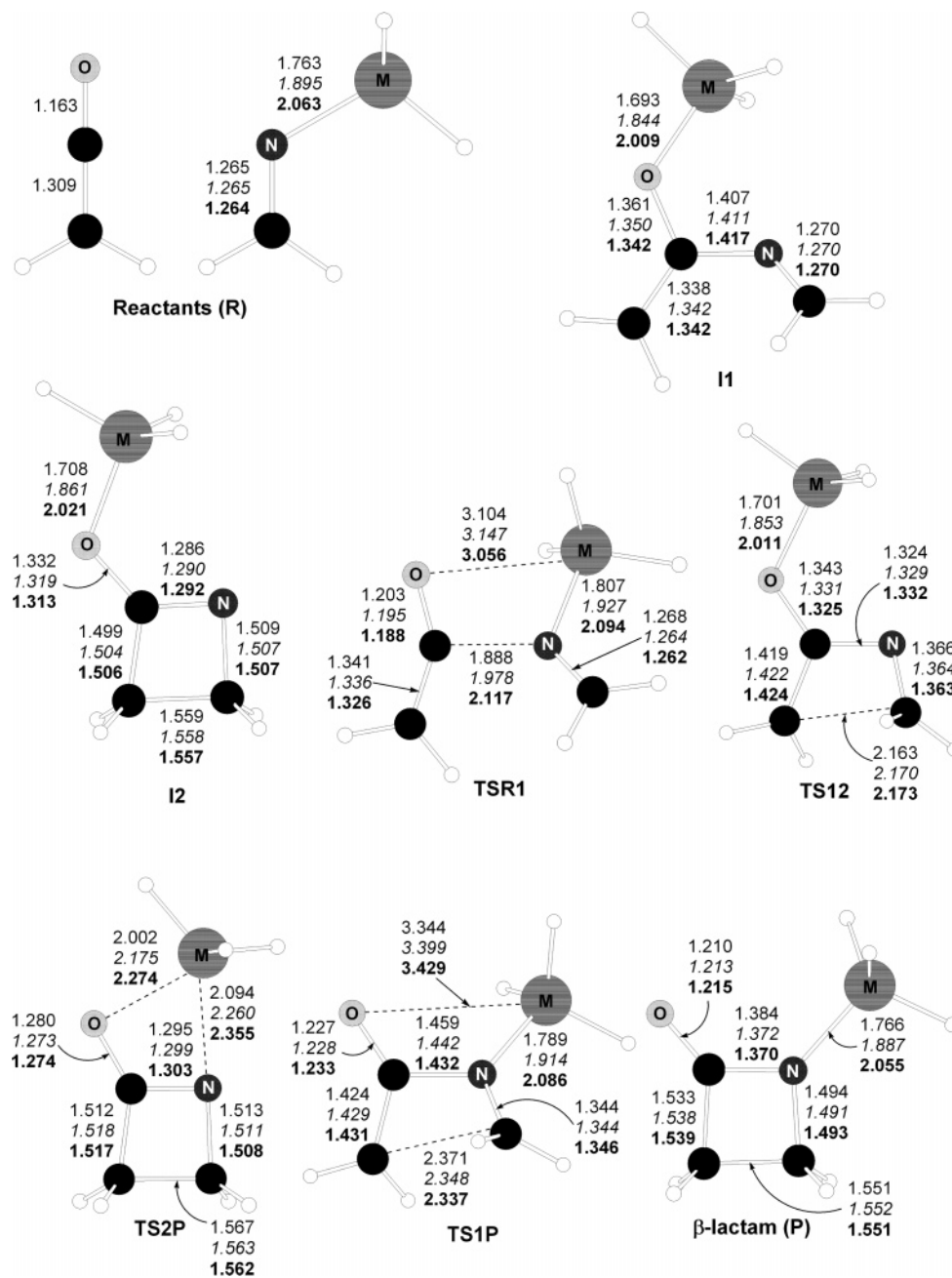


**Figure 1.** B3LYP geometries of all the critical structures located along the reaction coordinate for the reaction of ketene with *N*-silyl- (plain), *N*-germyl- (italic), and *N*-stannylimine (bold) optimized in solution. Distances are given in angstroms.

To take into account condensed-phase effects, we used a self-consistent reaction field (SCRf) model proposed for quantum

chemical computations on solvated molecules.<sup>14</sup> The solvent is represented by a dielectric continuum characterized by its

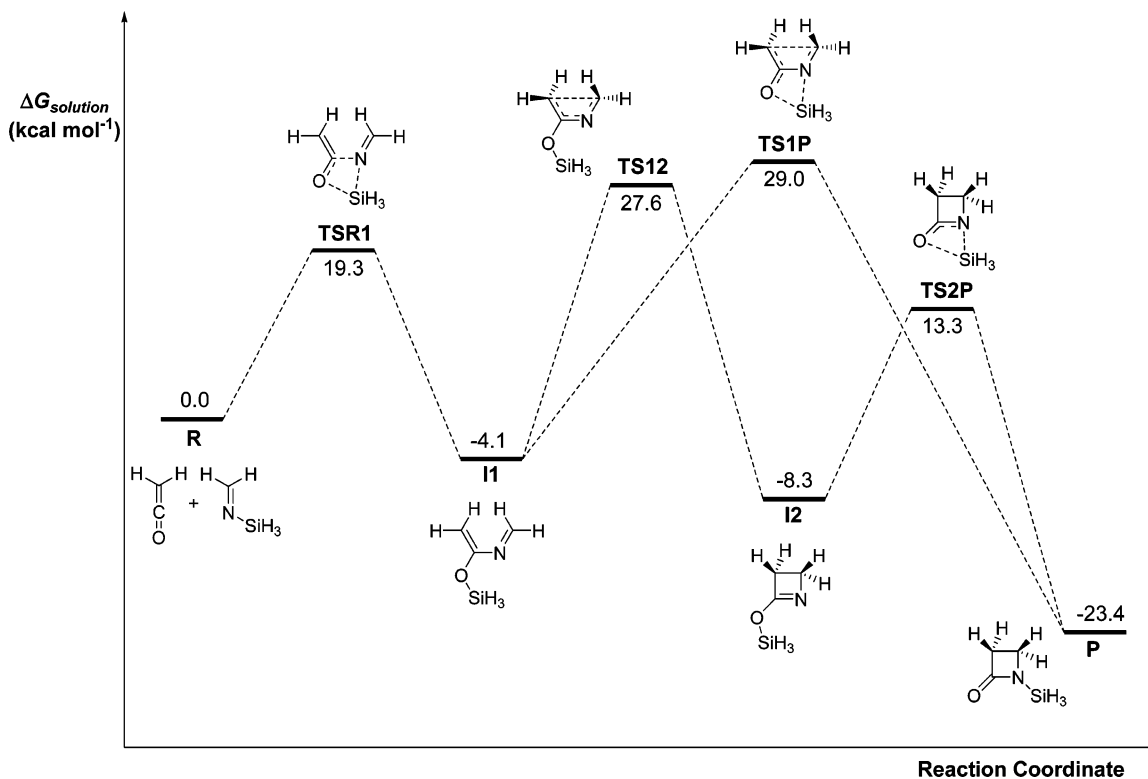


**Figure 2.** Relative Gibbs energy profiles in diethyl ether solution corresponding to the reaction between ketene and *N*-silylimine.

relative static dielectric permittivity  $\epsilon$ . The solute, which is placed in a cavity created in the continuum after spending some cavitation energy, polarizes the continuum, which in turn creates an electric field inside the cavity. This interaction can be taken into account using quantum chemical methods by minimizing the electronic energy of the solute plus the Gibbs energy change corresponding to the solvation process.<sup>15</sup> Addition to  $\Delta G_{\text{gas}}$  of the solvation Gibbs energy gives  $\Delta G_{\text{solution}}$ . Within the different approaches which can be followed to calculate the electrostatic potential created by the polarized continuum in the cavity we have employed the polarizable continuum model (PCM)<sup>16</sup> with the united atom Hartree–Fock (UAHF) parametrization.<sup>17</sup> The solvation Gibbs energies  $\Delta G_{\text{solvation}}$  along the reaction coordinate were evaluated through reoptimization of the geometry of all species in solution. A relative permittivity of 4.33 was employed to simulate diethyl ether as the solvent used in the experimental work. A natural population analysis on the species in solution was performed to obtain the corresponding atomic charges.<sup>18</sup>

## Results and Discussion

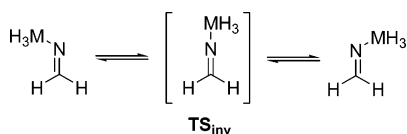
We will present now the results obtained for the cycloaddition reactions between ketene and *N*-silyl-, *N*-germyl-, and *N*-stannylimines. Table 1 collects the relative electronic energies and Gibbs energies in solution for the three reactions, and Figure 1 displays the most important geometrical features of all the critical structures located along the reaction coordinate optimized in solution. Tables 1S–3S of Supporting Information present the absolute and relative electronic energies, the ZPVE corrections, and the relative Gibbs energies in the gas phase and in diethyl ether solution for all the critical structures, and Figure 1S displays the geometrical parameters of all the critical structures optimized in the gas phase.

We found an analogous mechanism for the three processes investigated. We present in Figure 2 the energy profiles

corresponding to the ketene + *N*-silylimine reaction as an illustration. We will discuss in the text the Gibbs energy variation in solution along the reaction coordinates.

Initially the reactants evolve through the TS **TSR1** for the nucleophilic attack of the nitrogen lone pair of the imine on the carbonyl carbon atom of the ketene with the simultaneous migration of the  $\text{MH}_3$  group to yield the intermediate **I1**. The corresponding energy barriers are 19.3 (Si), 16.1 (Ge), and 13.4 kcal mol<sup>-1</sup> (Sn). **I1** is a 1,3-azadiene which in some cases has been isolated and characterized<sup>5</sup> and is 4.1 (Si), 1.9 (Ge), and 6.8 kcal mol<sup>-1</sup> (Sn) more stable than separate reactants. This intermediate **I1** can afford the final  $\beta$ -lactam through a two-step process. At the first TS, **TS12**, the closure of the  $\beta$ -lactam ring takes place to give the intermediate **I2** with an energy barrier of 31.7 (Si), 30.9 (Ge), and 31.3 kcal mol<sup>-1</sup> (Sn). In the second step the  $\text{MH}_3$  migration from the oxygen atom to the nitrogen atom occurs by transforming **I2** into the final product, **P**, which is 23.4 (Si), 24.2 (Ge), and 25.1 kcal mol<sup>-1</sup> (Sn) more stable than reactants. In contrast to previous theoretical studies we also found a concerted process leading from **I1** to **P** through the TS **TS1P** for the simultaneous  $\text{MH}_3$  migration and  $\beta$ -lactam ring closure with an energy barrier of 33.1 (Si), 27.7 (Ge), and 31.4 kcal mol<sup>-1</sup> (Sn). At these TSs **TS1P** the  $\text{MH}_3$  moiety presents a positive charge of 0.58–0.66 e which is quite similar to that in the final  $\beta$ -lactam (0.56–0.63 e). Accordingly, at these TSs the  $\text{MH}_3$  migration is practically completed, whereas the ring closure is just starting so that both processes are very asynchronous. Therefore, from the above results we see that in the case of *N*-germylimines the transformation of **I1** into the  $\beta$ -lactam takes place in a concerted manner, whereas for *N*-silylimines the ring closure and the  $\text{MH}_3$  migration occurs in a consecutive fashion and for *N*-stannylimines both routes are competitive.<sup>19</sup> The large value of the energy barriers impeding the evolution of **I1** both into the final product and back into

## SCHEME 3



the separate reactants in the case of *N*-silylimines is the reason this intermediate has been isolated and characterized experimentally.

It is interesting to note that the energy barrier for **TSR1** diminishes from Si to Sn. It appears then that the more polarizable the element M the more favorable the nucleophilic attack of the nitrogen lone pair on the ketene. In fact, the  $\text{MH}_3$  groups present in the corresponding imines important positive charges of +0.52 e for *N*-silyl and *N*-germylimines and of +0.57 e for *N*-stannylimine. At **TSR1**, the  $\text{MH}_3$  moiety presents an even larger positive charge of about 0.60–0.65 e in its migration to bond the oxygen atom, which has developed a negative charge because of the attack of the nitrogen lone pair on the ketene, and leaving a lone pair at the nitrogen atom giving then rise to a non-zwitterionic intermediate **II** ( $\mu \cong 2$  D) in contrast with the zwitterionic character of the classical Staudinger intermediate ( $\mu \cong 5$  D).

Concerning the second part of the reaction, we note that for *N*-germylimines the concerted mechanism is more favorable than the two-step one. This is a consequence of the effect of solvent, which in the three reactions considered by us favors the **TS1P**, although for *N*-stannylimines this effect just cancels the electronic energy difference between **TS1P** and **TS12**, and for *N*-silylimines cannot override the electronic energy trend (see Table 1).

In the three cases the rate-determining energy barrier corresponds to the evolution of **II** through **TS1P** or **TS12**. From Table 1 we see that the kinetically less favorable processes are those for *N*-silyl and *N*-stannylimines, whereas the most favorable one is that for *N*-germylimines by about 3 kcal mol<sup>-1</sup>. Thus, in the latter case the  $\beta$ -lactam could be obtained from the ketene and the *N*-germylimine in a domino process.

It has been previously established that the experimentally observed *trans*-stereoselectivity for the reaction of ketene and *N*-silylimine stems from the isomerization of the *N*-silylated imine through the inversion at the nitrogen atom that presents lower activation energy than the bond-forming steps. To discuss this possibility in the case of *N*-germyl and *N*-stannylimines, we have evaluated the energy barrier for the isomerization in these compounds (see Scheme 3) at the B3LYP/6-311+G(d,p) theory level using the LANL2DZ effective core potential for Ge and Sn and optimizing all the critical structures in diethyl ether solution. We see from Table 1 that not only for *N*-silylimines but also for *N*-germyl and *N*-stannylimines the energy barrier for these isomerizations is lower than the energy barriers for the formation of the azadiene intermediate **II**, and, consequently, in the last two processes the *trans*- $\beta$ -lactam would be also obtained.

In summary the reaction between ketene and *N*-germylimine is a two-step process due to the effect of solvent, whereas the cycloaddition of ketene and *N*-silylimine follows a three-step mechanism because in this case the evolution of the electronic energy along the reaction coordinate predominates over the effect of solvent. For *N*-stannylimine the two- and three-step mechanisms are competitive. In all the cases the rate-determining barrier corresponds to the transformation of the azadiene intermediate, **II**, through **TS1P** or **TS12**. The largest rate-determining barrier corresponds to the reaction of *N*-silyl and

*N*-stannylimines, whereas in the case of *N*-germylimine the energy barrier corresponding to **TS1P** is lower enough to render the  $\beta$ -lactam in a domino process. The cycloaddition of ketene and *N*-germylimine is kinetically the most favorable one. In the three cases the isomerization of the imine through the inversion at the nitrogen atom is easier than the formation of the azadiene intermediate so that the three processes would afford the *trans*- $\beta$ -lactam.

**Acknowledgment.** We thank Principado de Asturias for financial support (Grant PB02-045 FICyT). We also thank CIEMAT for computer facilities.

**Supporting Information Available:** Optimized structures in the gas phase, absolute and relative electronic energies, ZPVE corrections, and relative Gibbs energies in the gas phase and in diethyl ether solution for all the critical structures located in this work. This material is available free of charge via the Internet at <http://pubs.acs.org>.

## References and Notes

- (1) (a) Georg, G. I.; Ravikumar, V. T. In *The Organic Chemistry of  $\beta$ -lactams*; Georg, G. I., Ed.; VCH: New York, 1993; pp 295–368. (b) Palomo, C.; Aizpurua, J. M.; Ganboa, I.; Oiarbide, M. *Eur. J. Org. Chem.* **1999**, 3223, 3.
- (2) (a) Singh, G. S. *Tetrahedron* **2003**, 59, 7631. (b) Pelotier, B.; Rajzmann, M.; Pons, J.-M.; Campomanes, P.; López, R.; Sordo, T. L. *Eur. J. Org. Chem.* **2005**, 2599.
- (3) (a) Pacansky, J.; Chang, J. S.; Brown, D. W.; Schwarz, W. *J. Org. Chem.* **1982**, 47, 2233. (b) Moore, H. W.; Hughes, G.; Srinivasachar, K.; Fernández, M.; Nguyen, N. V.; Schoon, D.; Tranne, A. *J. Org. Chem.* **1985**, 50, 4231. (c) Lynch, J. E.; Riseman, S. M.; Laswell, W. L.; Tschaden, D. M.; Volante, R. P.; Smith, G. B.; Shinkay, I. *J. Org. Chem.* **1989**, 54, 3792.
- (4) (a) Sordo, J. A.; González, J.; Sordo, T. L. *J. Am. Chem. Soc.* **1992**, 114, 6249. (b) Cossío, F. P.; Ugalde, J. M.; López, X.; Lecea, B.; Palomo, C. *J. Am. Chem. Soc.* **1993**, 115, 995. (c) Cossío, F. P.; Arrieta, A.; Lecea, B.; Ugalde, J. M. *J. Am. Chem. Soc.* **1994**, 116, 2085. (d) Assfeld, X.; Ruiz-López, M. F.; González, J.; López, R.; Sordo, J. A.; Sordo, T. L. *J. Comput. Chem.* **1994**, 15, 479. (e) Assfeld, X.; López, R.; Ruiz-López, M. F.; González, J.; Sordo, T. L.; Sordo, J. A. *J. Mol. Struct. (THEOCHEM)* **1995**, 331, 1. (f) López, R.; Ruiz-López, M. F.; Rinaldi, D.; Sordo, J. A.; Sordo, T. L. *J. Phys. Chem.* **1996**, 100, 10600. (f) Fang, D. C.; Fu, X. Y. *Int. J. Quantum Chem.* **1996**, 57, 1107. (g) Arrieta, A.; Lecea, B.; Cossío, F. P. *J. Org. Chem.* **1998**, 63, 5869. (h) Truong, T. N. *J. Phys. Chem. B* **1998**, 102, 7877. (i) Bharatam, P. V.; Kumar, R. S.; Mahajan, M. P. *Org. Lett.* **2000**, 2, 2725. (j) Venturini, A.; González, J. *J. Org. Chem.* **2002**, 67, 9089. (k) Zhou, C.; Birney, D. M. *J. Am. Chem. Soc.* **2002**, 124, 5231.
- (5) (a) Bandini, E.; Martelli, G.; Spunta, G.; Bongini, A.; Panunzio, M. *Tetrahedron Lett.* **1996**, 37, 4409. (b) Martelli, G.; Spunta, G.; Panunzio, M. *Tetrahedron Lett.* **1998**, 39, 6257. (c) Bandini, E.; Favi, G.; Martelli, G.; Panunzio, M.; Piersanti, G. *Org. Lett.* **2000**, 2, 1077.
- (6) Bongini, A.; Panunzio, M.; Piersanti, G.; Bandini, E.; Martelli, G.; Spunta, G.; Venturini, A. *Eur. J. Org. Chem.* **2000**, 2379.
- (7) For the definition of consecutive and domino reactions see: Titze, L. F.; Beilfuss, V. *Angew. Chem., Int. Ed. Engl.* **1993**, 32, 131.
- (8) (a) Takahashi, M.; Kira, M. *J. Am. Chem. Soc.* **1999**, 121, 8597. (b) Takahashi, M.; Kira, M. *J. Am. Chem. Soc.* **1997**, 119, 1948.
- (9) (a) Becke, A. D. *J. Chem. Phys.* **1993**, 98, 5648. (b) Becke, A. D. *Phys. Rev. A* **1988**, 38, 3098. (c) Lee, C.; Yang, W.; Parr, R. G. *Phys. Rev. B* **1988**, 37, 785.
- (10) Wadt, W. R.; Hay, P. J. *J. Chem. Phys.* **1985**, 82, 284.
- (11) Frisch, M. J.; Trucks, G. W.; Schlegel, H. B.; Scuseria, G. E.; Robb, M. A.; Cheeseman, J. R.; Montgomery, J. A., Jr.; Vreven, T.; Kudin, K. N.; Burant, J. C.; Millam, J. M.; Iyengar, S. S.; Tomasi, J.; Barone, V.; Mennucci, B.; Cossi, M.; Scalmani, G.; Rega, N.; Petersson, G. A.; Nakatsuji, H.; Hada, M.; Ehara, M.; Toyota, K.; Fukuda, R.; Hasegawa, J.; Ishida, M.; Nakajima, T.; Honda, Y.; Kitao, O.; Nakai, H.; Klene, M.; Li, X.; Knox, J. E.; Hratchian, H. P.; Cross, J. B.; Bakken, V.; Adamo, C.; Jaramillo, J.; Gomperts, R.; Stratmann, R. E.; Yazyev, O.; Austin, A. J.; Cammi, R.; Pomelli, C.; Ochterski, J. W.; Ayala, P. Y.; Morokuma, K.; Voth, G. A.; Salvador, P.; Dannenberg, J. J.; Zakrzewski, V. G.; Dapprich, S.; Daniels, A. D.; Strain, M. C.; Farkas, O.; Malick, D. K.; Rabuck, A. D.; Raghavachari, K.; Foresman, J. B.; Ortiz, J. V.; Cui, Q.; Baboul, A. G.; Clifford, S.; Cioslowski, J.; Stefanov, B. B.; Liu, G.; Liashenko, A.; Piskorz, P.; Komaromi, I.; Martin, R. L.; Fox, D. J.; Keith, T.; Al-Laham, M. A.; Peng, C. Y.; Nanayakkara, A.; Challacombe, M.; Gill, P. M. W.;



Johnson, B.; Chen, W.; Wong, M. W.; Gonzalez, C.; Pople, J. A. *Gaussian 03*, Revision B.04; Gaussian, Inc.: Wallingford, CT, 2004.

(12) (a) González, C.; Schlegel, H. B. *J. Chem. Phys.* **1989**, *90*, 2154. (b) González, C.; Schlegel, H. B. *J. Phys. Chem.* **1990**, *84*, 5523.

(13) *Statistical Mechanics*; McQuarrie, D. A., Ed.; Harper & Row: New York, 1976.

(14) (a) Rivail, J. L.; Rinaldi, D.; Ruiz-López, M. F. In *Theoretical and Computational Model for Organic Chemistry*, Vol. 339; NATO ASI Series C; Formosinho, S. J., Csizmadia, I. G., Arnaut, L., Eds.; Kluwer Academic Publishers: Dordrecht, The Netherlands, 1991. (b) Cramer, C. J.; Truhlar, D. G. In *Reviews in Computational Chemistry*; Lipkowitz, K. B., Boyd, D. B., Eds.; VCH: New York, 1995. (c) Rivail, J. L.; Rinaldi, D. In *Computational Chemistry: Review of Current Trends*; Leszczynski, J., Ed.; World Scientific: New York, 1996. (d) Cramer, C. J.; Truhlar, D. G. *Chem. Rev.* **1999**, *99*, 2161.

(15) Claverie, P. In *Quantum Theory of Chemical Reactions*; Daudel, R., Pullman, A., Salem, L., Veillard, A., Eds.; Reidel: Dordrecht, The Netherlands, 1982.

(16) (a) Tomasi, J.; Persico, M. *Chem. Rev.* **1994**, *94*, 2027. (b) Tomasi, J.; Cammi, R. *J. Comput. Chem.* **1995**, *16*, 1449.

(17) Barone, V.; Cossi, M.; Tomasi, J. *J. Chem. Phys.* **1997**, *107*, 3210.

(18) (a) Reed, A. E.; Weinhold, F. *J. Chem. Phys.* **1985**, *83*, 735. (b) Reed, A. E.; Curtiss, L. A.; Weinhold, F. *Chem. Rev.* **1988**, *88*, 899.

(19) To assess the validity of our results concerning the comparison between ordinary basis sets and pseudopotentials, we have reoptimized both in gas-phase and in solution all of the energy profiles for the reaction of *N*-germylimine (see Tables 1 and 3S). These results clearly indicate a good performance of the LANL2DZ pseudopotential compared with the 6-311+G\*\* basis set. The Gibbs energy barriers in solution obtained through optimization with the 6-311+G\*\* basis set are quite similar to those obtained with LANL2DZ: the difference in Gibbs energy between **TS1P** and **TS12** is 1.9 kcal mol<sup>-1</sup> with the pseudopotential and 2.3 kcal mol<sup>-1</sup> with the 6-311+G\*\* basis set, thus confirming that for the reaction between ketene and *N*-germylimine the most favorable mechanism from **II** is the concerted one.